Golf swing simulation and carry distance prediction from smartphone motion capture estimates

Anand Jain, Huy Nguyen, Rishabh Gokhale & Rahul Mohari
Cupertino, CA 95014, USA

Abstract

Double-pendulum models of the golf swing are well established in sports-science literature, yet most studies focus on either theoretical dynamics or expensive motion capture. We present an open-source pipeline that (1) uses OpenCap's video analysis to extract shoulder torque, (2) forward-simulates a subject-specific double-pendulum model in the Julia programming language package ModelingToolkit.jl, and (3) augments the swing model with a ball-trajectory model to predict carry distance. We validate our pipeline with comparisons to known carry distances and clubhead velocities. This flexible, low-cost approach lowers the barrier for amateur golfers, coaches, and biomechanics researchers to explore model variants and ultimately optimize swing mechanics outside of specialized labs.

1 Introduction

Traditional estimation of golf-swing kinematics from motion capture is prohibitively expensive for all but professionals due to the cost of motion capture systems and the time required for experts to manually track position markers (Uhlrich et al., 2023). This work builds on top of advances made in computer vision for kinematics estimation to drive a player-specific double-pendulum swing model and a ball-trajectory model. This addresses the gap between hobbyist understanding and theoretical tools by giving players easily understood metrics on their swing, including airborne distance (carry) and club-head speed. The Lagrangian double-pendulum has been a canonical and central model in golf-swing dynamics modeling since 1970 (Jorgensen, 1970). The ModelingToolkit package in the Julia programming language offers a way to construct and compose differential equation models (Ma et al., 2021). We provide an open-source implementation of the Lagrangian double-pendulum model and a ball-trajectory model in ModelingToolkit that is flexible and modular, allowing for modifications and extensions (Jain, 2025).

2 Background

Our work enables players to film their golf swing and use it to drive a carry distance prediction model. Figure 1 demonstrates a block diagram view of the components of our work.

2.1 Swing model

Figure 1: A block diagram of our pipeline

Table 1: Double Pendulum Model Table

Code Symbol	Paper Symbol	Name	Unit	Value
`t`	t	Time	s	0
`th1(t)`	θ_1	Shoulder angle from vertical	rad	$-\frac{\pi}{2}$
`om1(t)`	ω_1	Shoulder rotational velocity	rad s^{-1}	0
`th2(t)`	θ_2	Wrist angle from vertical	rad	$-\pi$
`om2(t)`	ω_2	Wrist rotational velocity	rad s^{-1}	0
`l1`	l_1	Arm length	m	0.7
`m1`	m_1	Arm mass	kg	1.6
`l2`	l_2	Club length	m	1.1
`m2`	m_2	Club mass	kg	0.34
`g`	g	Gravitational acceleration	m s^{-2}	9.81
`tau_sh`	τ_{shoulder}	Maximum shoulder torque	m^2 kg s^{-2}	80
`tau_wr`	τ_{wrist}	Maximum wrist torque	m^2 kg s^{-2}	30

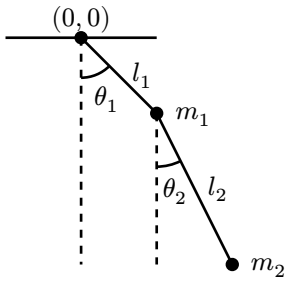

Figure 2: The Double Pendulum model

We begin our work by reviewing the classical mechanics of the forced double pendulum, which is the most widely used model for golf-swing kinematics (Betzler et al., 2008). We then introduce our ball trajectory model.

The notation used in the equations will match Figure 2 and Table 1. We use single and double pendulum equations to generate shoulder and wrist motions. The usage of point masses is discussed in Section 5. The equations of motion are derived using the forced Euler-Lagrange equations.

$$\begin{gathered} L = T - V \\ \frac{\partial L}{\partial \theta_i} - \left(\frac{\mathrm{d}}{\mathrm{d}t} \frac{\partial L}{\partial \dot{\theta}_i} \right) = Q_i(t) \end{gathered} \tag{1}$$

T is the kinetic energy of the system and V is the potential energy, θ_i are the dependent variables of the system, $\dot{\theta}_i$ are the angular velocities of the pendulum (also referenced as ω_i) and Q_i is the forcing function on θ_i.

The initial conditions $(\theta_i(0), \omega_i(0))$ of our base swing model can be found in Jorgensen (1970), the arm length and mass are from de Leva (1996), the shoulder torque τ_{shoulder} can be found in Pickering and Vickers (1999), the wrist torque is from Sprigings and Neal (2000). Driver club mass and length are readily found online.

We begin with the unforced single point-mass pendulum, which has the following Lagrangian and equations of motion.

$$L_{\text{single}} = -g * l_1 * m_1 * (1 - \cos(\theta_1(t))) + 0.5(l_1^2) * m_1 * (\omega_1(t)^2) \tag{2}$$

```
Differential(t)(om1(t)) ~ ((Q(t))[1] - g*l1*m1*sin(th1(t))) / ((l1^2)*m1)
Differential(t)(th1(t)) ~ om1(t)
```

The single pendulum model is overly simplistic and requires unrealistic shoulder torques to reach typical clubhead velocities (see Section 4).

Now we introduce the canonical double pendulum model. The full written Lagrangian and differential equations are meant for reference but not interpretability. Review the code in Jain (2025) for the full derivation. The Lagrangian is

```
function double_pendulum_lagrangian((om1, om2), (th1, th2), (l1, m1, l2,
m2, g), t)
    v1_sq = l1^2 * om1^2
    v2_sq = v1_sq + l2^2 * om2^2 + 2 * l1 * l2 * om1 * om2 * cos(th1 - th2)

    # kinetic
    T = (1 / 2) * (m1 * v1_sq + m2 * v2_sq)

    y1_from_rest = l1 * (1 - cos(th1))
    y2_from_rest = y1_from_rest + l2 * (1 - cos(th2))

    # potential
    V = g * (m1 * y1_from_rest + m2 * y2_from_rest)
    T - V
end
```

$$L_{\text{double}} = T - V \tag{3}$$

The differential equations are long; see Section A for the full equations of motion.

The Cartesian coordinates of the masses $\{(x_1, y_1), (x_2, y_2)\}$ as well as their component velocities $\{(\dot{x_1}, \dot{y_1}), (\dot{x_2}, \dot{y_2})\}$, the wrist velocity and the clubhead velocity $\{v_1, v_2\}$ are derived quantities from the dependent variables of the system. Coordinates are relative to the origin, taken to be the pivot of the first mass (shoulder joint).

$$\begin{aligned}
x_1 &= l_1 \sin(\theta_1) \\
y_1 &= -l_1 \cos(\theta_1) \\
x_2 &= x_1 + l_2 \sin(\theta_2) \\
y_2 &= y_1 - l_2 \cos(\theta_2) \\
\dot{x_1} &= l_1 \cos(\theta_1)\dot{\theta_1} \\
\dot{y_1} &= l_1 \sin(\theta_1)\dot{\theta_1} \\
\dot{x_2} &= l_1 \cos(\theta_1)\dot{\theta_1} + l_2 \cos(\theta_2)\dot{\theta_2} \\
\dot{y_2} &= l_1 \sin(\theta_1)\dot{\theta_1} + l_2 \sin(\theta_2)\dot{\theta_2} \\
v_1 &= \sqrt{\dot{x_1}^2 + \dot{y_1}^2} \\
v_2 &= \sqrt{\dot{x_2}^2 + \dot{y_2}^2}
\end{aligned} \tag{4}$$

We now discuss the methodology for determining the clubhead speed (v_2) at the time of collision. We incorporate a "callback" in the differential equation integrator that will perform a root finding routine to calculate the exact time when $\theta_1 = \theta_2$. Callback and event-handling functionality are built into the ModelingToolkit package. This condition corresponds to the point where the club and arms are aligned. A limitation of this approach is that for most initial conditions and forcing torques, there is no guarantee that the collision condition will be satisfied at the point where the ball is. Guaranteeing that the stopping condition occurs at $(0, -(l_1 + l_2))$ in Cartesian coordinates would require solving for the torques that would produce this condition. This is known as a shooting problem for boundary value problems and could be addressed in the future (Ascher et al., 1995).

2.2 Momentum Transfer

The transfer of momentum from the club to the ball in our model is governed by elastic collision. The velocity of the ball can be calculated by solving the system of equations that relates the conservation of momentum and conservation of kinetic energy. If m_1 and v_1 are the mass and velocity of the clubhead, and m_2 and v_2 are the mass and velocity of the ball, we can then obtain the following system of equations. We assume the ball has zero velocity before impact, and v_1' and v_2' are the velocities after collision.

$$\begin{aligned} \frac{1}{2}m_1v_1^2 + \cancel{\frac{1}{2}m_2v_2^2} &= \frac{1}{2}m_1v_1'^2 + \frac{1}{2}m_2v_2'^2 \\ m_1v_1 + \cancel{m_2v_2} &= m_1v_1' + m_2v_2' \end{aligned} \tag{5}$$

The solution set will include a trivial solution, where $v_1 = v_1'$. The other solution provides us with the true final velocities. We then use the club-specific loft angle and the magnitude of v_2' as the initial condition of the trajectory model. The assumption of elastic collision is discussed in Section 5.

2.3 Trajectory Model

A trajectory model was created to predict the airborne carry distance of the ball given the initial velocity magnitude as a result of an elastic collision. The specific club used determines the horizontal and vertical components of this vector. Two model variants are compared, one in which the only force acting on the ball is gravity, and another in which drag slows the acceleration of the ball proportional to the velocity. In Section 4 we analyze the validity of these two models.

$$\begin{aligned} \dot{x} &= v_x \\ \dot{v_x} &= 0 \\ \dot{y} &= v_y \\ \dot{v_y} &= -g \end{aligned} \tag{6}$$

The inclusion of a drag term proportional to velocity leads to the following system.

$$\begin{aligned} \dot{x} &= v_x \\ \dot{v_x} &= -kvv_x \\ \dot{y} &= v_y \\ \dot{v_y} &= -kvv_y - g \end{aligned} \tag{7}$$

Table 2: Trajectory Model Table

Symbol	Name	Unit	Value
x	Horizontal position	m	Initialized to 0
y	Vertical position	m	Initialized to 0
v_x	Horizontal velocity	$\frac{m}{s}$	Initialized to $v_0 \cos(\theta)$
v_y	Vertical position	$\frac{m}{s}$	Initialized to $v_0 \sin(\theta)$
θ	Loft angle	rad	Club specific
v_0	Initial ball velocity magnitude	$\frac{m}{s}$	Simulation specific
v	Instantaneous ball velocity	$\frac{m}{s}$	$\sqrt{v_x^2 + v_y^2}$
k	Drag constant	m^{-1}	0.0052[1]
g	Gravitational Constant	$\frac{m}{s^2}$	9.81

We now detail the process whereby we extract shoulder torques from video that drive the models.

3 Data Acquisition and Processing

We used the open-source applications OpenCap and OpenSim to capture and analyze the mechanics of the golf swing (Uhlrich et al., 2023). OpenCap uses two cameras recording simultaneously to estimate 3D joint positions and segment motions during the swing. The process begins with camera calibration using a checkered board, which helps determine the cameras' parameters by defining their position and orientation relative to each other. The subject is then analyzed in a resting position, with height and weight specified to scale the subject's musculoskeletal model. After calibration, the subject is recorded performing a golf swing. This was done multiple times, both with and without a golf club, and from various angles to ensure the best possible results. The captured swing is then processed to generate detailed biomechanical data, including body movement and joint angles. This motion data is imported into OpenSim, an open-source software that replays motion data and can simulate the musculoskeletal system (Seth et al., 2018). The usage of OpenSim for more extensive analysis of how muscles, joints, and forces contribute to the golf swing by performing inverse kinematics is reserved for future work.

In the following plots, the downswing begins at approximately $t = 3.5$ seconds and lasts for a few hundred milliseconds.

[1](Jenkins et al., 2018)

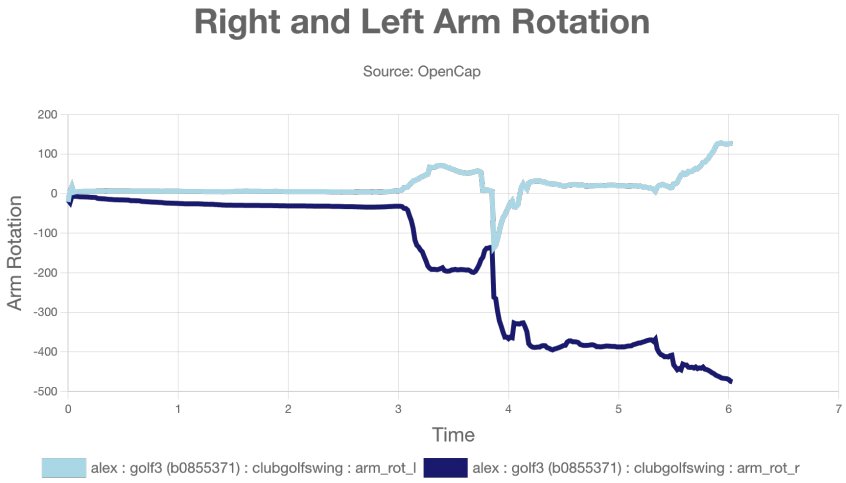

Figure 3: Arm Rotation: Internal/external shoulder rotation

This graph shows the right and left arm rotation. Arm rotation is the circular movement of the arm at the shoulder joint, involving both internal and external rotation. The light blue line is the left arm, and the dark blue line is the right arm.

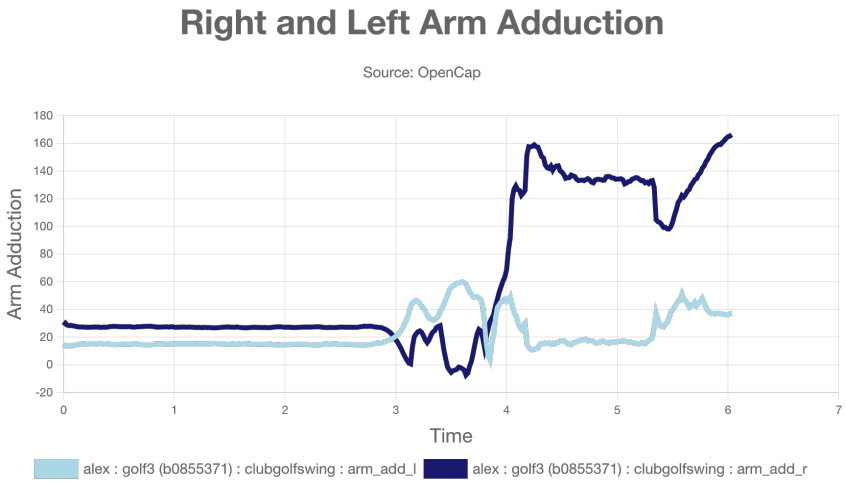

Figure 4: Arm Adduction: Arm toward/away from side (shoulder adduction)

This graph shows the right and left arm adduction. Arm adduction is the movement of the arm towards the body. The light blue line is the left arm, and the dark blue line is the right arm.

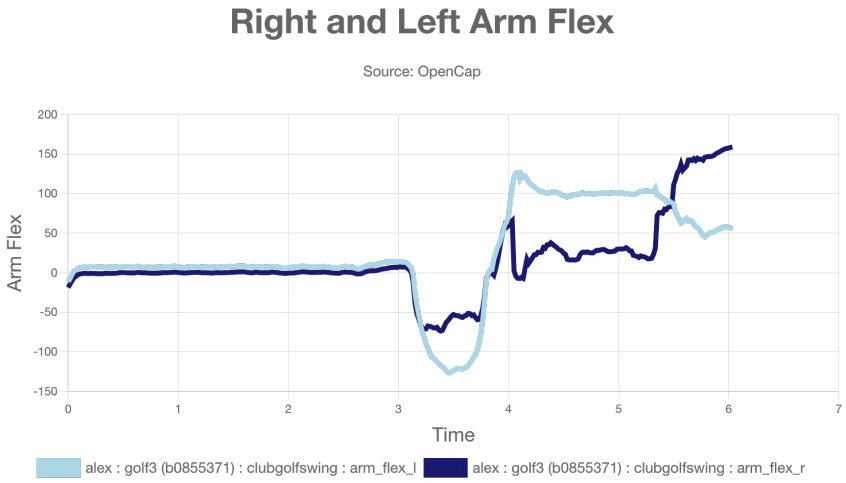

Figure 5: Arm Flex: Arm forward/backward lift (shoulder flexion)

This graph shows the right and left arm flex. Arm flex is the movement of bending the arm at the shoulder joint, bringing the upper arm forward and upward. The light blue line is the left arm, and the dark blue line is the right arm.

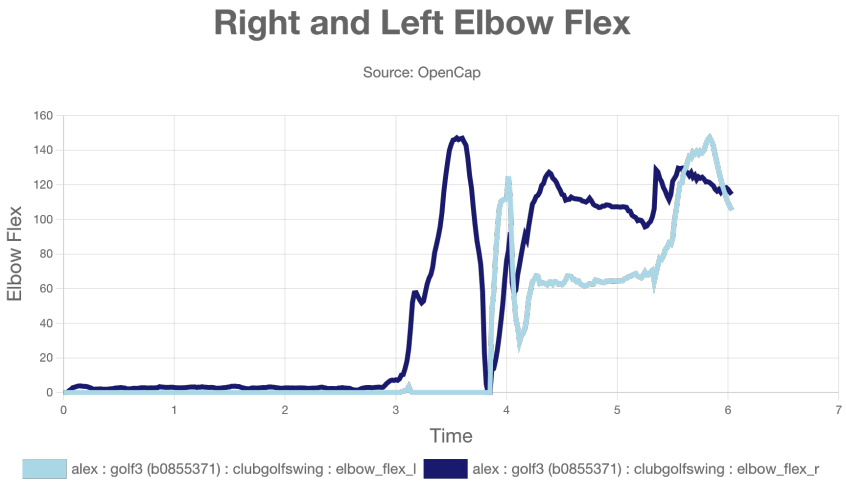

Figure 6: Elbow Flex: Elbow bending (Elbow flexion)

This graph shows the right and left elbow flex. Elbow flex is the movement that decreases the angle between the forearm and the upper arm, bending the elbow. The light blue line is the left arm, and the dark blue line is the right arm.

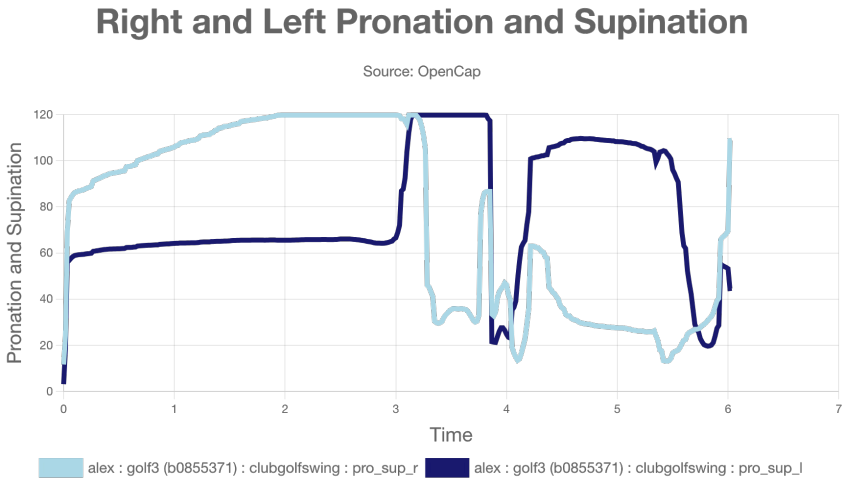

Figure 7: Pronation and Supination: Forearm rotation (For wrist)

This graph shows the right and left pronation and supination over time. Pronation is the rotation of the forearm so that the palm faces down (or back), while supination is the rotation of the forearm so that the palm faces up (or forward). The light blue line is the left arm, and the dark blue line is the right arm.

OpenCap and OpenSim, while powerful tools for motion capture and biomechanical analysis, have limitations that can affect the accuracy of golf swing simulations. OpenCap relies on a video-based neural network (OpenPose) to estimate joint positions, which can introduce errors in joint angles, segment orientations, and joint center locations—especially for small or complex movements like those of the wrist or fingers (Cao et al., 2019). Factors such as camera angle, distance, lighting, and background can further impact calibration accuracy. These inaccuracies carry over to OpenSim, where the musculoskeletal models may not faithfully reflect an individual's anatomy, particularly for joints like the shoulder or spine that are critical in golf. As a result, any errors in motion data from OpenCap can directly affect the reliability of kinematic and dynamic outputs from OpenSim.

The extraction of shoulder torque from these graphs is computed via finite differencing on the time series. We compute the torque by the product of the angular acceleration and the moment of inertia. A standard 2.7 kg uniformly distributed arm is used for computing the moment. For a right-handed golfer, the left arm stays mostly straight for the entirety of the downswing so we only used the data of the arm-flex. As is evident from the swing data produced from OpenCap, much more than arm-flex is used to drive the club into the ball. However, to simplify our model, we rely solely on torque estimation using arm flex.

We compute the following estimates for the max torque of each shoulder of our subject from OpenCap in Table 3. These torques are used to drive the simulation.

Table 3: Torque estimates from OpenCap

Name	**Torque**
"arm_flex_l" torque	90.2 N m
"arm_flex_r" torque	146.9 N m

We can see the swing as a strobe plot in Figure 9. We compare the clubhead velocity graphs in Figure 8.

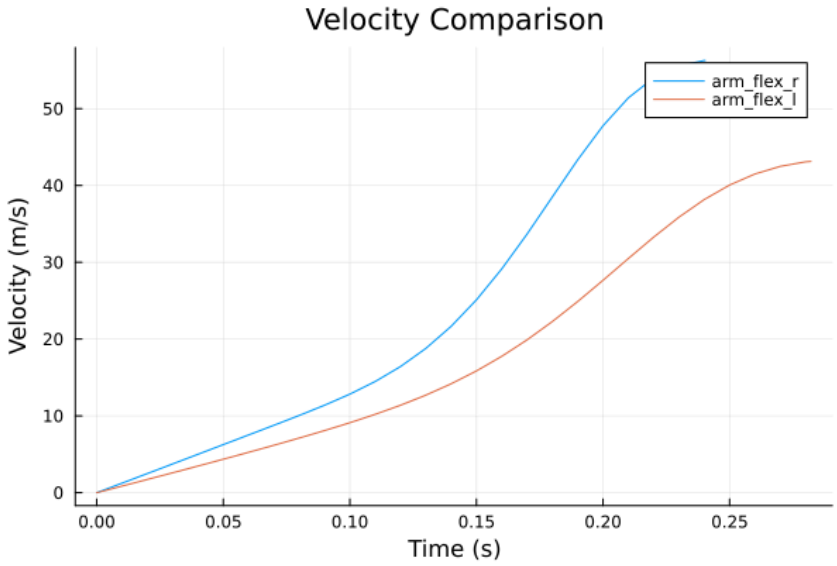

Figure 8: Instantaneous clubhead velocities of two simulations of the double pendulum swing model driven by the torque estimates of Table 3

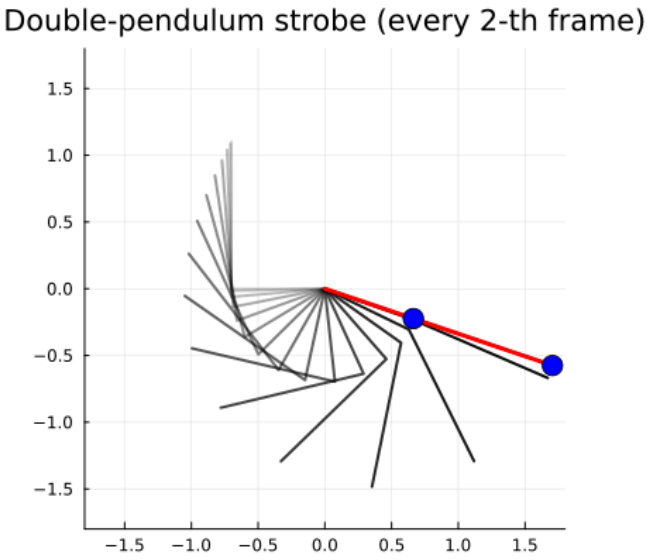

Figure 9: Subject swing simulation seeded from "arm_flex_l" torque estimate

4 Model Validation, Results, and Analysis

Simulations are conducted using the Julia DifferentialEquations.jl package (Rackauckas and Nie, 2017). The methodology for running the joint swing-trajectory simulations is as follows. The full model definition for `swing` and `trajectory` can be found in the GitHub repository (Jain, 2025). The variables `swing_updates` and `traj_updates` are parameter sets that override the defaults already recorded in the model structure.

```
swing_updates = [l1 => 0.63, l2 => 1.14, m2 => 0.32, tau_sh => 30, tau_wr
=> 10]
prob = ODEProblem(swing, swing_updates, (0, 1000))
swing_sol = solve(prob; saveat=0.01)
```

```
clubhead_v = swing_sol[sqrt(v2_sq)][end]
defs = merge(ModelingToolkit.defaults(swing), swing_updates)
club_v, ball_v = compute_elastic_collision(defs[m2], clubhead_v, ball_mass)
traj_updates = [v0 => ball_v, k => kdrag, loft => deg2rad(10)]
prob2 = ODEProblem(trajectory, traj_updates, (0, 1000))
traj_sol = solve(prob2; saveat=0.01)
```

We first demonstrate how the single pendulum model is overly simplified. Figure 10 shows the simulation of a single pendulum driven by 300 Nm of shoulder torque and produces ≈ 50 m/s of clubhead velocity. While this clubhead speed is realistic of experienced players, the torque has never been recorded experimentally.

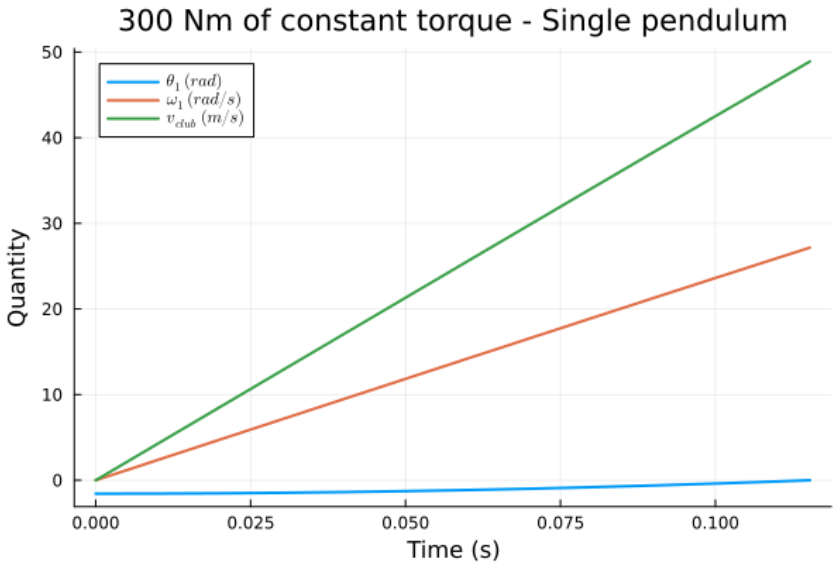

Figure 10: Simulating the Single Pendulum model driven with 300Nm of torque

In order to validate the double pendulum model, we create a set of three fictitious subjects of increasingly desirable parameters for maximum carry distance. The three parameter sets are simulated and we qualitatively discuss the accuracy of the predictions (Table 4). A comprehensive analysis of different tiers of players' shoulder and wrist torques, along with the associated clubhead velocity and carry distance was not found in academic literature. Table 4 data was collected from a mix of blogs and academic papers. The most useful of which can be found at TrackMan Golf Blog (2025) for amateurs and Tang and Abraham (2003) for professional players.

Table 4: Fictitious estimates of different parameter sets for increasingly skilled golfers

Metric	**Amateur**	**Intermediate**	**Professional**
Arm length (m)	0.63	0.63–0.65	0.65
Clubhead speed (m/s)	41.6–42.1	46.9–49.2	51.41
Shoulder torque (N · m)	30	40	100
Wrist torque (N · m)	10–11	15	35
Ball speed (m/s)	59.46	67.06	76.25
Carry distance (m)	182.88	219.46	256.03
Total distance (m)	195.56	237.74	267.20

An end-to-end comparison is performed whereby input shoulder and wrist torque drive both the swing and trajectory model, using elastic collision for the transfer of energy from

club to ball. Table 5 provides us with confidence that aspects of our modeling are sane. Drag always decreases carry distance and increased shoulder and wrist torque cause the ball to carry further. Notably, for the professional simulation without drag we obtain a carry-distance of 239m. This is low but not completely unreasonable compared to reality, which is approximately 300m including roll (Tang and Abraham, 2003). We can attribute this error to using a loft of 10 degrees for the driver (Table 6). In reality, backspin on the ball causes it to lift and achieve a higher effective loft. We also notice a consistent under-prediction in clubhead speed and ball speed given the torque. We believe that this can be attributed to the weakness of the double pendulum model. A golfer typically has a third rigid link at the right elbow that begins bent at the start of the downswing but extends throughout. A reference for a triple pendulum swing model can be found in Tang and Abraham (2003). This additional torque would improve the accuracy of predictions.

Table 5: Simulation of 6 sets of parameters for joint swing and ball simulation

Simulation Name	**Clubhead Velocity (m/s)**	**Ball Velocity (m/s)**	**Carry Distance (m)**
Amateur (No Drag)	28	49.1	84.2
Amateur (Drag)	28	49.1	66
Intermediate (No Drag)	31.5	55.2	106
Intermediate (Drag)	31.5	55.2	79
Professional (No Drag)	47.2	82.7	239
Professional (Drag)	47.2	82.7	138

Figure 11 depicts the trajectories for the simulation of the subject-specific data of the left arm. Note that wrist torque is not recorded by OpenCap; thus we supplement the simulation of our subject-specific model with a general "intermediate" skill level wrist torque of a constant 15 N·m. We see that our predictions for the subject-specific model arrive in the ballpark of a typical drive.

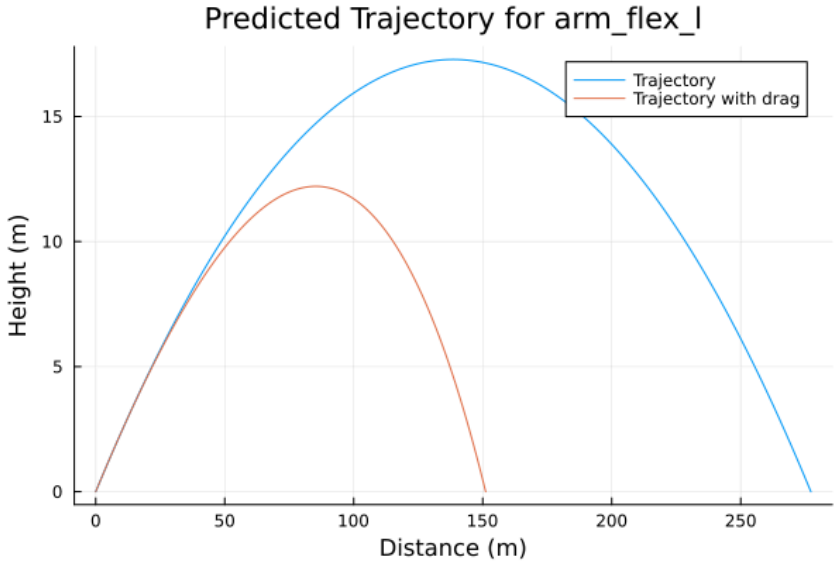

Figure 11: Subject carry distance seeded with "arm_flex_l" torque using a standard[2] value of $k = 0.0052m^{-1}$ for golf ball drag coefficient and with $k = 0$.

5 Limitations and Assumptions

5.1 Simple Body Mechanics

In our model, we treated the wrist and shoulder mechanics as simple, rigid linkages, but in reality most clubs flex back and forth, which adds more velocity to the ball at impact. Although we get reasonable results and approximations, real-world scenarios are more complex.

Future Improvements:

- Integrate the full-body musculoskeletal model in OpenSim.
- Improve the pipeline to provide more actionable feedback on swing inefficiencies
- Analyze different torque profiles acting on the shoulder and wrist to better approximate the behavior of real muscle.

5.2 Ball Aerodynamics

Our trajectory model does not account for the lift of the ball. Lift depends on factors like spin, air density, and velocity, which complicate the dynamics of the projectile motion. By simplifying the aerodynamics of the ball, the results of our model are less accurate, but helps us focus on the basic projectile motion and estimation of carry-distance.

Future Improvements:

- Add Magnus lift into our model to make projectile motion more accurate, this can help players better understand the physics of ball flight .
- Show how different clubs affect spin and change shot dynamics.

5.3 Inelastic Collisions

Collision with the club and ball leads to loss of energy due to heat and compression of the ball. For our model, collisions are elastic, where there is no energy loss. Real collisions are not governed by this simple assumption.

Future Improvements:

- Take into account the energy loss when the club strikes the ball.
- Simulate COR as a function of impact speed and location.
- Study the effects of club and ground contact.
- Include ball deformation (Hooke's Law)

5.4 Environmental Factors

Our model strictly predicts carry distance, but players typically are interested in total shot distance. On the course, there are external environmental factors that affect the path of the ball, such as wind, trees, water, humidity, and more, that add a level of unpredictability. For our model, we kept the surface flat and planar to simplify predicting carry distance.

Future Improvements:

- Simulate rolling after the impact of the ball on the ground.
- Add different surfaces, air resistance, wind direction, and grass/terrain types.

5.5 Player Fatigue

[2](Jenkins et al., 2018)

As a golfer plays and continues to swing and hit the ball multiple times, they will most definitely begin to fatigue, affecting how hard and or accurately they strike the ball. By giving the model no fatigue over time, it allows the model to focus on the pure biomechanics of the movement and the resulting ball flight, making the results more consistent.

Future Improvements:

- Record how hitting the ball multiple times and other factors affect a golfer over time.

5.6 Motion of Ball

In our model, the ball's trajectory is simplified onto a two-dimensional plane, ignoring side-to-side movement. We are also keeping a consistent launch height, although golf balls are not hit at the same angle and position. By keeping the launch height consistent, we focus on other variables, such as swing speed or club type, without introducing added complexity from varying launch conditions.

Future Improvements:

- Simulate a 3-D model and take into account if the ball goes straight or if it fades, slices, hooks, pulls, pushes, draws, and cuts.
- Introduce differing launch heights and angles.

5.7 Point Masses in Pendulum Models

In both the arm and the club, there are different moments of inertia that influence how they rotate and transfer energy during the swing. We have decided to concentrate the mass into one spot in order to remove the mass distribution from the arm to the club, simplifying the derivation of the equations of motion.

Future Improvements:

- Include moments of inertia for a more realistic simulation of rotational motion of the arm and club that would better resemble actual biomechanics.

6 Conclusion

Our aim was to assess whether smartphone motion capture and a simple carry distance model would provide reasonable predictions under standard swing conditions. We estimated the shoulder torque from motion capture data to drive a carry distance differential equation system. We found that even the simplified double pendulum and projectile motion models have predictive value in achieving reasonable distances for standard shoulder and wrist torques. We hope that our work can be adopted as a standard reference model that is easy to simulate and modify by coaches, hobbyists, and biomechanics researchers.

Author Contributions

All authors conceived of the project plan and design of the work jointly.
Anand Jain and **Huy Nguyen** jointly worked to derive single and double pendulum dynamics.
Anand Jain wrote the code, performed the modeling, simulation, and data analysis, and drafted and revised the manuscript, including tables and figures. Helped with presentation.
Huy Nguyen Collected OpenCap video data and 3-D muscle-skeletal model, and analyzed swing data in OpenSim. Provided manuscript drafting and revising. Helped with presentation.
Rishabh Gokhale Provided format for paper and data of golfers while solving rolling equations, provided manuscript drafting and revising. Helped with the presentation.
Rahul Mohari created the presentation and helped research.

References

Ascher, U. M., Mattheij, R. M. M., and Russell, R. D. *Numerical Solution of Boundary Value Problems for Ordinary Differential Equations*. SIAM, 1995.

Betzler, N., Monk, S., Otto, S., and Shan, G. From the double pendulum model to full-body simulation: Evolution of golf swing modeling. *Sports Technology*, *1*, 175–188, 2008. https://doi.org/10.1002/jst.60

Cao, Z., Hidalgo Martinez, G., Simon, T., Wei, S., and Sheikh, Y. A. OpenPose: Realtime Multi-Person 2D Pose Estimation using Part Affinity Fields. *IEEE Transactions on Pattern Analysis and Machine Intelligence*, 2019.

de Leva, P. Adjustments to Zatsiorsky-Seluyanov's segment inertia parameters. *Journal of Biomechanics*, *29*(9), 1223–1230, 1996. https://doi.org/https://doi.org/10.1016/0021-9290(95)00178-6

Golf Monthly. *What Are the Degree Lofts of Golf Clubs?*, 2024. https://www.golfmonthly.com/gear/clubs/degree-loft-golf-clubs

Hireko Golf. *Modern Guide to Golf Club Fitting: Weight and Weight Distribution*, 2023. https://www.hirekogolf.com/weight-distribution-guide

Jain, A. *anandijain/GolfModel.jl: v0.1.0*. Zenodo, 2025, June. https://doi.org/10.5281/zenodo.15725743

Jenkins, P. E., Arellano, J., Ross, M., and Snell, M. Drag Coefficients of Golf Balls. *World Journal of Mechanics*, *8*(6), 236–241, 2018. https://doi.org/10.4236/wjm.2018.86019

Jorgensen, J., Theodore. On the Dynamics of the Swing of a Golf Club. *American Journal of Physics*, *38*(5), 644–651, 1970. https://doi.org/10.1119/1.1976419

Ma, Y., Gowda, S., Anantharaman, R., Laughman, C., Shah, V., and Rackauckas, C. *ModelingToolkit: A Composable Graph Transformation System For Equation-Based Modeling*, 2021.

Pickering, and Vickers. On the double pendulum model of the golf swing. *Sports Engineering*, *2*(3), 161–172, 1999. https://doi.org/https://doi.org/10.1046/j.1460-2687.1999.00028.x

Rackauckas, C., and Nie, Q. DifferentialEquations.jl–a performant and feature-rich ecosystem for solving differential equations in Julia. *Journal of Open Research Software*, *5*(1), 2017.

Seth, A., Hicks, J. L., Uchida, T. K., Habib, A., Dembia, C. L., Dunne, J. J., Ong, C. F., DeMers, M. S., Rajagopal, A., Millard, M., Hamner, S. R., Arnold, E. M., Yong, J. R., Lakshmikanth, S. K., Sherman, M. A., Ku, J. P., and Delp, S. L. OpenSim: Simulating Musculoskeletal Dynamics and Neuromuscular Control to Study Human and Animal Movement. *PLOS Computational Biology*, *14*(7), 1–20, 2018. https://doi.org/10.1371/journal.pcbi.1006223

Sprigings, E., and Neal, R. An Insight into the Importance of Wrist Torque in Driving the Golfball: A Simulation Study. *Journal of Applied Biomechanics*, *16*, 356–366, 2000. https://doi.org/10.1123/jab.16.4.356

Tang, W.-T., and Abraham, L. D. *ANALYSIS OF GOLFSWING OPTIMIZATION MODELS*, 2003. https://api.semanticscholar.org/CorpusID:202544250

TrackMan Golf Blog. *PERFORMANCE OF THE AVERAGE MALE AMATEUR GOLFER*, 2025.

Uhlrich, S. D., Falisse, A., Kidziński, Ł., Muccini, J., Ko, M., Chaudhari, A. S., Hicks, J. L., and Delp, S. L. OpenCap: Human movement dynamics from smartphone videos. *PLOS Comput. Biol.*, *19*(10), 1–26, 2023. https://doi.org/10.1371/journal.pcbi.1011462

United States Golf Association. *Equipment Rules*, 2023. https://www.usga.org/content/dam/usga/pdf/2019/usga-equipment-rules.pdf

A Appendix

The full forced Lagrangian double pendulum equations of motion in Julia.

```
Differential(t)(th2(t)) ~ om2(t)

Differential(t)(th1(t)) ~ om1(t)

Differential(t)(om2(t)) ~ ((Q(t))[2] + (-l1*((Q(t))[1] + g*(-
l1*m1*sin(th1(t)) - l1*m2*sin(th1(t))) - l1*l2*m2*(om2(t)^2)*sin(-th2(t) +
th1(t)))*l2*m2*cos(-th2(t) + th1(t))) / (0.5(2(l1^2)*m1 + 2(l1^2)*m2)) -
g*l2*m2*sin(th2(t)) + l1*l2*m2*(om1(t)^2)*sin(-th2(t) + th1(t))) / ((-
(l1^2)*(l2^2)*(m2^2)*(cos(-th2(t) + th1(t))^2)) / (0.5(2(l1^2)*m1 +
2(l1^2)*m2)) + (l2^2)*m2)

Differential(t)(om1(t)) ~ ((Q(t))[1] + (-l1*((Q(t))[2] + (-l1*((Q(t))[1] +
g*(-l1*m1*sin(th1(t)) - l1*m2*sin(th1(t))) - l1*l2*m2*(om2(t)^2)*sin(-
th2(t) + th1(t)))*l2*m2*cos(-th2(t) + th1(t))) / (0.5(2(l1^2)*m1 +
2(l1^2)*m2)) - g*l2*m2*sin(th2(t)) + l1*l2*m2*(om1(t)^2)*sin(-th2(t) +
th1(t)))*l2*m2*cos(-th2(t) + th1(t))) / ((-(l1^2)*(l2^2)*(m2^2)*(cos(-
th2(t) + th1(t))^2)) / (0.5(2(l1^2)*m1 + 2(l1^2)*m2)) + (l2^2)*m2) + g*(-
l1*m1*sin(th1(t)) - l1*m2*sin(th1(t))) - l1*l2*m2*(om2(t)^2)*sin(-th2(t) +
th1(t))) / (0.5(2(l1^2)*m1 + 2(l1^2)*m2))
```

Table 6: A Typical 14-Club Set.[3]

Club	**Loft (°)**	**Length (m)**	**Mass (kg)**
Driver	10	1.14	0.32
3-Wood	15	1.09	0.33
5-Wood	19	1.07	0.34
3-Hybrid	21	1	0.37
4-Hybrid	24	1.02	0.37
5-Iron	27	0.965	0.41
6-Iron	31	0.953	0.41
7-Iron	35	0.927	0.41
8-Iron	39	0.914	0.41
9-Iron	44	0.902	0.41
PW	48	0.889	0.41
AW	52	0.889	0.42
SW	56	0.889	0.42
Putter	4	0.864	0.56

[3]Data compiled from: (Golf Monthly, 2024), (United States Golf Association, 2023), (Hireko Golf, 2023).